Coherent beam combination of two slab laser amplifiers based on stochastic parallel gradient descent algorithm

Xiao Li (李 霄)*, Xiaolin Dong (董小林), Hu Xiao (肖 虎), Xiaolin Wang (王小林), and Xiaojun Xu (许晓军)**

College of Opticelectric Science and Engineering, National University of Defense Technology, Changsha 410073, China

**Corresponding author: crazy.li@163.com; **corresponding author: xuxj@21cn.com*

Received March 2, 2011; accepted April 21, 2011; posted online July 11, 2011

Coherent beam combination (CBC) of laser arrays is an efficient way to scale brightness. We demonstrate CBC of two slab laser amplifiers based on active phase locking. Instead of the complex phase detection system, intensity detection is used and the feedback control signal is calculated based on the stochastic parallel gradient descent (SPGD) algorithm. The experimental investigation on a 101.5-W CBC of two slab amplifiers shows that the entire system in a closed loop performs well for long-time observation. A combination efficiency of nearly 81% is realized. The slab amplifier laser arrays are the coherent beams efficiently combined by active phase locking based on the SPGD.

OCIS codes: 140.0140, 140.3298.
doi: 10.3788/COL201109.101401.

Coherent beam combination (CBC) of laser arrays has potential applications in laser radar and energy delivering systems[1]. Two categories of CBC are passive phasing in a master oscillator and active phasing using power amplifier configuration[2−9]. Most studies on CBC are based on fiber lasers because of their inherently compact size and high beam quality. In 2009, Northrop Grumman Corporation (NGC) unveiled their 100-kW system based on slab laser amplifiers with heterodyne phase detecting technology[10]. To date, this system remains an excellent example of the highest power demonstrations of CBC.

Compared with the complex phase detection system, intensity detection is more readily available[11]. However, the feedback cannot be used to directly control the phase array, so that a special algorithm is necessary[12−16]. To our knowledge, no reports on CBC with bulk or rod lasers based on intensity detection have been published. In this letter, we demonstrate CBC of two slab lasers based on the stochastic parallel gradient descent (SPGD) algorithm. The experimental investigation on a 101.5-W CBC of two slab amplifiers shows that the entire system in a closed loop performs well for long-time observation. Nearly 80% combining efficiency is realized.

Figure 1 shows a schematic of the experimental setup. The master oscillator (MO) provides the continuous-wave (CW) seed laser with single frequency and linear polarization. After passing through a fiber laser pre-amplifier and splitter, the energy of the beam is equally distributed into two slab power amplification (PA) systems, one of which has a phase modulator (PM) in front. The laser beams is amplified to about 9 W and then outputted. To ensure beam quality, the entire fiber laser consists of a single-mode all-fiber element.

The Gaussiam beams outputted from the fiber laser are reshaped to elliptical beams and transmitted into the slab after passing through a polarizer. The configuration of the four-pass slab laser amplifier is shown in Fig. 2.

The main gain module comprises two end-pumped conduction-cooled slab lasers with Nd:YAG crystal medium. The size of the slab is 1.7×11×67 (mm), whose ends are diffusion-bonded with undoped YAG end caps and cut at 45° with anti-reflection (AR) coating at 1 064 nm. A special coating is used on the two largest surfaces to guarantee the total internal reflection of the zigzag reflection optic path. The 808-nm pump lasers are coupled into the slab on each of the end-coupling areas with AR coating. To maintain beam quality, the total pump power should be below 500 W for each slab, from which about 50-W power can be extracted. After collimation, the amplified lasers are combined and transmitted together.

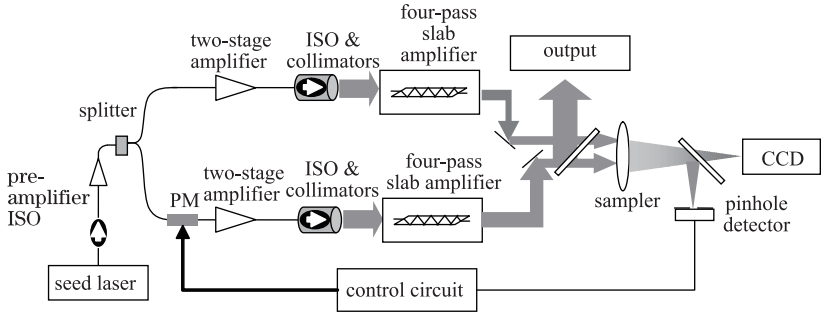

Fig. 1. Schematic of the experimental system.

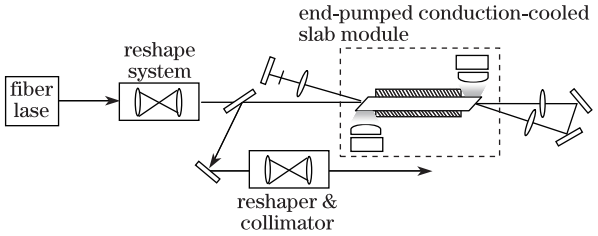

Fig. 2. Schematic of the four-pass slab laser amplifier.

To obtain the control signal for phase locking, the output laser should be sampled (less than 1%) and focused onto a detector with a pinhole in front, whose size is a little less than the main lobe of the focused beam. Using a special algorithm, the control signal can be computed and fed back to the PM array. Therefore, the energy distribution, observed using a CCD camera, is optimized if the convergence process is sufficiently fast to compensate for the phase noise.

The SPGD algorithm is used for active phasing. The metric function is $J(u)$, where u is the control signal applied to the phase modulator. By controlling u with the SPGD algorithm, the maximal value of J is acquired and the coherent combination approach is applied to the ideal value. The algorithm is implemented in infinite iterations and then manually terminated. Each iteration cycle works as follows. 1) Statistically independent random perturbations are generated and converted to voltage δu, which is a small value; 2) the control voltages are applied on the phase modulators with the positive perturbations. Metric function $J^+ = J(u + \delta u)$ is obtained from the detector, and then the control voltages with the negative perturbations are applied. Subsequently, metric function $J^- = J(u - \delta u)$ is obtained; 3) the gradients of metric function J (defined as the intensity of main-lobe detected by the photo-detector) with function $\delta J = J^+ - J^-$ are estimated; 4) the control voltage $u = u + \gamma \delta u \delta J$ is updated, where γ is the update gain, and $\gamma > 0$ accords with the procedure of maximization in CBC.

In the absence of active phase control, because of the phase fluctuations inside the laser medium, the interference pattern keeps shifting and metric function J is time variant. Once the SPGD algorithm is implemented, i.e., the entire system is in a closed loop, the intensity pattern at the observation plane should be clear and steady. The long-exposure far-field intensity distribution indicates that the peak intensity visibly increases (Figs. 3(a) and (b)), which is normalized to the same peak intensity. Figure 3(c) is the vertical section of the long-exposure intensity distribution in Figs. 3(a) and (b). The contrast of the coherent-combined beam profile in Fig. 3(c) is about 81%. The fringe contrast is defined by the formula $(I_{\max} - I_{\min})/(I_{\max} + I_{\min})(I_{\max} - I_{\min})/(I_{\max} + I_{\min})$, where $I_{\max}$ and $I_{\min}$ are the maximum optical intensity and adjacent minimum on the intensity pattern, respectively.

The time-dependent signals of energy encircled in the pinhole are shown in Fig. 4(a). According to the figure, the peak intensity of the far-field pattern is improved by a factor of 1.6 after the loop is closed. In an ideal situation, the factor should be 2. The primary reason for the loss

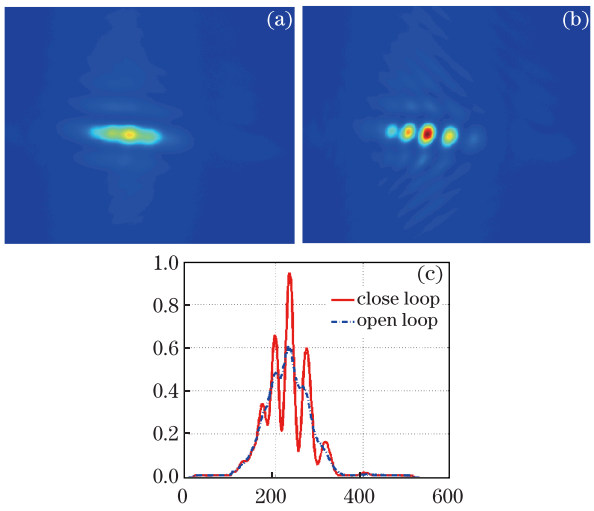

Fig. 3. Long-exposure far-field intensity distribution (about 7 s). (a) Open loop (normalized); (b) closed loop (normalized); (c) distribution vertical section.

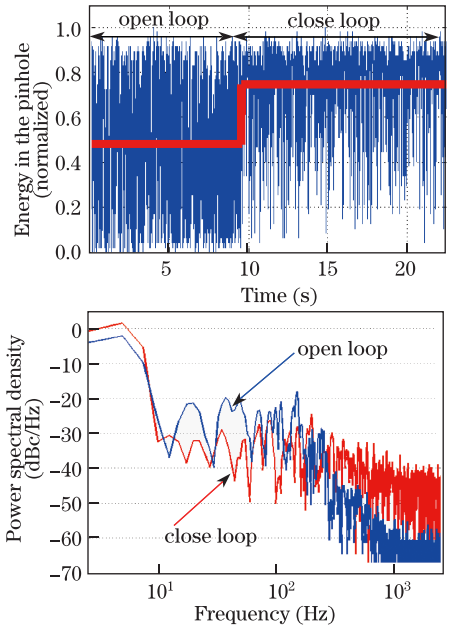

Fig. 4. Varying of the energy in the pinhole. (a) Time variations; (b) frequency spectra.

of coherent efficiency is that the wave-front aberration caused by the slab lasers and the optic element induce the intensity disturbance of the far-field distribution. As shown in Figs. 3(b) and (c), the far-field pattern appears aberrant and dissymmetrical, thereby decreasing the peak intensity.

The fidelity of CBBC and the phase fluctuation suppression result can be further studied by calculating the frequency spectrum of the time-series signal of the power encircled in the pinhole (Fig. 4 (b)). The power fluctuating at the frequency of several hundred hertz is efficiently controlled by the SPGD algorithm.

In conclusion, we demonstrate CBC of two slab amplifiers with a total 101.5-W output power using the digital signal processing (DSP)-based SPGD algorithm. The peak intensity of the far field improves by a factor of 1.6

and the contrast of the coherent-combined beam profile is about 81% when the system is in a closed loop. The primary factor contributing to the loss of coherent efficiency is the wave-front aberration caused by the slab lasers and optic element.

This work was supported by the Innovation Foundation for Graduates in National University of Defense Technology (No. B090704) and the Hunan Provincial Innovation Foundation for Postgraduates (No. CX2009B006). The authors were indebted to Professor J. Zhou, Dr. Y. Qi, Dr. C. Liu, and Ms. Y. Ding of the Shanghai Institute of Optics and Fine Mechanics, Chinese Academy of Sciences for their help in designing, developing, and assembling the fiber amplifiers.

References

1. T. Y. Fan, IEEE J. Sel. Topics Quantum Electron. **11,** 567 (2005).
2. J. E. Kansky, C. X. Yu, D. V. Murphy, S. J. Shaw, R. C. Lawrence, and C. Higgs, Proc. SPIE **6306,** 63060G (2006).
3. Y. M. Huo, P. K. Cheo, and G. G. King, Opt. Express **12,** 6230 (2004).
4. A. Shirakawa, T. Saitou, T. Sekiguchi, and K. Ueda, Opt. Express **10,** 1167 (2002).
5. G. D. Goodno, H. Komine, S. J. McNaught, S. B. Weiss, S. Redmond, W. Long, R. Simpson, E. C. Cheung, D. Howland, P. Epp, M. Weber, M. McClellan, J. Sollee, and H. Injeyan, Opt. Lett. **31,** 1247 (2006).
6. J. Anderegg, S. Brosnan, E. Cheung, P. Epp, D. Hammons, H. Komine, M. Weber, and M. Wickham, Proc. SPIE **6102,** 61020U (2006).
7. R. Xiao, J. Hou, M. Liu, and Z. Jiang, Opt. Express **16,** 2015 (2008).
8. K. Gao, L. Xu, R. Zheng, G. Chen, H. Zheng, and H. Ming, Chin. Opt. Lett. **8,** 45 (2010).
9. W. Wang, Q. Lou, B. He, J. Zhou, Z. Li, Y. Xue, and X. Liu, Chin. Opt. Lett. **8,** 490 (2010).
10. J. Marmo, H. Injeyan, H. Komine, S. McNaught, J. Machan, and J. Sollee, Proc. SPIE **7195,** 719507 (2009).
11. P. Zhou, Z. Liu, X. Wang, Y. Ma, H. Ma, and X. Xu, Appl. Phys. Lett. **94,** 231106 (2009).
12. P. Zhou, Y. Ma, X. Wang, H. Ma, X. Xu, and Z. Liu, Opt. Lett. **34,** 2939 (2009).
13. P. Zhou, Z. Liu, X. Wang, Y. Ma, H. Ma, X. Xu, and S. Guo, IEEE J. Sel. Top. Topics Quantum Electron. **15,** 248 (2009).
14. P. Zhou, X. Wang, Y. Ma, J. Leng, H. Ma, J. Wang, X. Xu, and Z. Liu, J. Phys. B **42,** 195401 (2009).
15. Y. Ma, X. Wang, J. Leng, H. Xiao, X. Dong, J. Zhu, W. Du, P. Zhou, X. Xu, L Si, Z. Liu, and Y. Zhao, Opt. Lett. **36,** 951 (2011).
16. Y. Ma, P. Zhou, X. Wang, H. Ma, X. Xu, L. Si, Z. Liu, and Y. Zhao, Opt. Lett. **35,** 1308 (2010).